Journal of Theoretical and Applied Information Technology
15th April 2018. Vol.96. No 7

ISSN: 1992-8645 www.jatit.org E-ISSN: 1817-3195

FAST MULTIFRACTAL EDGE DETECTION USING ANISOTROPIC DIFFUSION

[1]RAWAN ZAGHLOUL, [2]HAZEM HIARY, [3]MOH'D BELAL AL-ZOUBI
The University of Jordan, Amman 11942, Jordan
E-mail: [1]rawanzaghloul@yahoo.com, [2]hazemh@ju.edu.jo, [3]mba@ju.edu.jo

ABSTRACT

Image edge detection is a core operation in image processing applications. Classical approaches make use of fixed neighborhood detectors, while recent research recommends the incorporation of scale factor in filter design to increase both the accuracy of classifying edge pixels, and to provide more flexibility in retrieving multilevel edge maps. Multifractal approach follows this trend of incorporating the scale in feature analysis, and it is widely used in image analysis and pattern recognition applications. However, very few researches explore the abilities of multifractals in image edge map generation due to its extensive computation time which is a major obstacle in this research area. Herein, we propose AD-MED; a fast multifractal edge detector based on anisotropic diffusion filter. The evaluation of the proposed edge detector was done first qualitatively by visual assessment. Second, quantitatively in terms of both the quality of the results and the execution time. Experimental simulation shows that AD-MED outperforms the well-known multifractal edge detectors in both terms.

Keywords: *Fractals, Multifractal Analysis, Anisotropic Diffusion, Multilevel Edge Detection, Regularization Filters.*

1. INTRODUCTION

Image edge detection is a core operation in various image processing applications. It is the operation of extracting edges constituted by abrupt changes in color intensity or brightness of an image. An operator for edge detection is called: edge detector, and the result of an edge detector is called: edge map. Thus, edge map is a kind of image by which edges are emphasized and smooth regions are suppressed [1, 2].

Despite the fact that edge maps boost wide range of applications such as image enhancement, restoration [3], segmentation [4, 5], recognition [6], registration, and data hiding. Past research in edge detectors reveals that the problem of locating edges in real and natural images is a hard problem.

Classical methods in edge detection make use of gradient operators to discriminate edges, such as Sobel, Prewitt, and Robert's [7], these methods are extremely sensitive to noise. The success of an edge detection algorithm depends on its capability to produce good localized edge maps with minimal effect of noise.

However, noise is inherent in real images. Thus, to reduce the effect of noise, various edge detection methods suggest a smoothing step using low pass filters prior to edge detection step [8].

Difficulties raised from the smoothing step such as: how it could be tuned so it can both preserve fine edges and omit the effect of noise. Herein, some researches introduced a way to tackle this problem by using multiscale filters [9]. Such approach involves using smoothing operators at multiple scales, finding edge maps in every scale, and then combining the results to produce a final edge map. The main problem of this approach is how to combine the resulted edge maps to generate a final map [10].

The incorporation of scale factor initiates a new class of edge detectors that could increase both the accuracy of classifying edge pixels, and the flexibility of an edge detector so it can be tuned to retrieve multilevel edge maps [11-14].

Other researches have explored the use of multifractal analysis in edge description [15] where edge points are described by analyzing the

ISSN: 1992-8645 www.jatit.org E-ISSN: 1817-3195

regularity over multiple scales of pixel's neighborhood [16].

However, despite the powerful results of this approach in pattern recognition applications [17], it has received very little attention as an edge detection methodology; this is due to its high execution time, its manual thresholding which is mostly used for generating a final edge map, and its tendency to produce some undesirable artefacts in the obtained results.

Therefore, the scope of this paper is confined to a set of multifractal methods that we have considered as relevant with respect to the multifractal edge detection (MED) problem, namely: Min-MED, Max-MED, Mean-MED, OSC-MED, and Edge-MED.

The aims of this paper are two-fold. First, to provide efficient and effective multifractal model dedicated to image edge detection. Second, to highlight the abilities of the new trend of multilevel edge detection. Indeed, recent research supports the idea of incorporating scale factor in filter design. Our concern in this paper is therefore to demonstrate this concept, and to show how it would be possible to use multifractal analysis in the context of multilevel edge detection.

Particularly, we propose a multifractal edge detector based on anisotropic diffusion filter. Which is both, more efficient compared to the specified MEDs, and more effective in a sense, that it generates a high-quality edge map that can be automatically thresholded.

The rest of this paper is organized as follows: Section 2 provides a brief background about anisotropic diffusion filter, fractals, and multifractal analysis. Section 3 discusses the proposed approach in edge detection. Section 4 introduces the experimental results and comparisons. Section 5 summarizes the contributions and significance of work. Finally, Section 6 concludes the paper.

2. BACKGROUND

2.1 Anisotropic Diffusion

The anisotropic diffusion (AD) filter was proposed in 1990 by Perona and Malik [11]. It is one of the popular image regularization filters, which is based on partial derivatives equations in which it applies the diffusion law on pixel intensity values to smooth an image [3].

This filter preserves edges in the image using a threshold function that is used to prevent the occurrence of diffusion across edges. This makes it very useful to preserve edges while removing noise or regularizing an image region.

The AD is an iterative filter and while increasing its number of iterations the image becomes smoother. It is defined as the local divergence around each pixel in the image such as [11, 18]

$$AD = \frac{\partial I(x,y,t)}{\partial t} = div(g(\|E\|)\mathrm{E}), \quad (1)$$

where *div* is the divergence operator, $E = \nabla I(x,y,t)$ is the gradient of a pixel located at position (x,y) in the image I at time t, and $g(.)$ is a conductance function that is chosen to satisfy the following conditions: 1) At the uniform interior region:

$$\lim_{x \to 0} g(x) = 1 \quad (2)$$

2) At the boundaries (edges):

$$\lim_{x \to 0} g(x) = 0 \quad (3)$$

For $g(x)$, two functions were proposed in [11], such as:

$$g_1(\mathrm{x}) = e^{-(x/K)^2} \quad (4)$$

$$g_2(x) = \frac{1}{1 + \left(\frac{x}{K}\right)^2} \quad (5)$$

where K is a constant that controls the diffusion rate and serves as a soft threshold between the image gradients that are attributed to noise and those attributed to edges. It is worth to mention that during our work in this paper we have used g_2 for AD filter.

Figure 1 shows an example of applying AD filter on an image.

Journal of Theoretical and Applied Information Technology
15th April 2018. Vol.96. No 7

ISSN: 1992-8645 www.jatit.org E-ISSN: 1817-3195

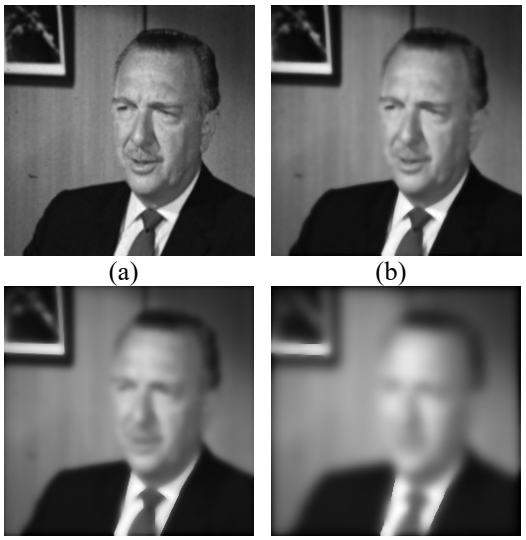

Figure 1: Applying AD Filter on 'Man' Image [19]. a) Original Image. b) The Results of Applying AD with 4 Iterations. c) 20 Iterations. d) 70 Iterations.

2.2 Fractals

In the past, the focus of mathematics was directed to regular sets and smooth functions to which the classical methods of calculus take a place. However, recent researches were directed toward the study of irregularities. That is because it provides a better understanding for the natural phenomena. Hence, a shift toward the mathematics of irregular sets and non-smooth functions becomes important. Herein, Fractal geometry provides a general framework for the study of such irregular sets [20].

The term 'fractal' was first introduced by Mandelbrot [21]. The importance of fractals lies in their geometric characteristic which gives a great ability to model natural objects such as clouds borders, forms of coastlines, mountain boarders, etc. Fractal is a mathematical notion that can describe continuous nowhere differentiable functions, surfaces, or curves. As we shall discuss, the idea of fractal geometry is closely related to the concepts of scale invariance and self-similarity [22].

According to Mandelbrot's definition of ideal fractal, it is a structure that possesses the property of exact self-similarity under all scales [23]. In other words, ideal fractal is composed of perfectly similar copies of itself, each scaled down by a constant factor, and they have to be organized in a way so to construct the original shape exactly. Figure 2 shows an example of generating the well-known fractal structure 'Sierpinski triangle', it is generated by recursively repeating a procedure of connecting the midpoints of each side of the equilateral triangle to form four separate triangles, and cutting out the triangle in the center, the figure shows three iterations of the process [24].

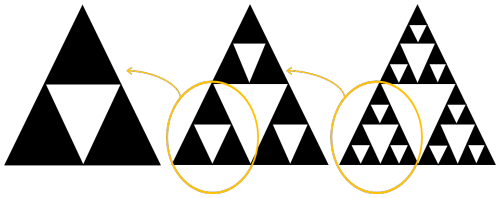

Figure 2: Self-similarity in Sierpinski Triangle.

Beside ideal fractals, a much broader conception about them was introduced by Mandelbrot in his paper 'How long is the coast of Britain?' [25]. His conception was to model nature in a way that actually captures roughness.

Fractal geometry differs from calculus, the latter assumes that functions (or shapes) tend to look smooth as you zoom in enough. But from Mandelbrot's perspective, this assumption is overly idealized and yields models that ignore fine details. Thus, Mandelbrot observed that self-similar shapes are good basis to model the regularity in some forms of roughness. But the popular perception that fractals only include perfectly self-similar shapes is another over idealization. Therefore, a general definition of fractals was developed based on the concept of fractal dimension, which defines how the mass of a shape changes while scaling it as depicted in eq.6.

$$\text{Mass scaling factor} = (\text{shape scaling factor})^{d} \quad (6)$$

For example, by scaling down the Sierpinski triangle to half of its area, its mass would be scaled down by a factor of one third, this means $(1/3)=(1/2)^{d}$. In this case, d is a fraction equals to $\log_2(3)\approx 1.585$, and hence it is called a fractal dimension fd. Therefore, Fractals can be defined as shapes whose dimension is not an integer but instead some fractional number. For grayscale images, fd is a scalar value that refers to how a grid of boxes fills the space under different scales of magnification where a higher fd value refers to a rough image surface. Meanwhile, a smaller fd value refers to a smooth image surface [26].

2.3 Multifractal Analysis

The multifractal approach is a generalization of fractals where a single fractal dimension is not enough to describe an image. In

ISSN: 1992-8645 www.jatit.org E-ISSN: 1817-3195

such case, a set of fractal dimensions are computed locally in the image space to generate what is called a local fractal map (or multifractal map).

A multifractal map is computed by finding the local fractal dimension (*lfd*) for each pixel in the image. Practically, for an image I of size $m \times n$, the above definition of local fractal map generation can be approximated by applying the following steps:

1. Convolve the image I with a specific kernel K multiple times for multiple scales of K. At each convolution step store the image generated from each scale. The result is a set of images ($M^1, M^2, ..., M^L$), where L denotes the number of chosen scales.

2. For each pixel $I_{x,y}$, create a feature vector whose length is the same as the number of the adopted scales. It consists of the intensity values at position (x,y) in all the images generated in step 1.

3. For each pixel $I_{x,y}$, draw a *log – log* plot between the adopted scales and the intensity values contained in the feature vector.

4. Create an $m \times n$ local fractal map whose pixels are determined by finding the slope of the best fitted line of the pixel's plot created in step 3.

5. Rescale the resulted map in the range [0-255] for better visualization.

Figure 3 shows an example of generating a multifractal map for the image in figure 1(a) using Mean kernel. Throughout the paper, we refer to the process of generating a multifractal edge map using a specific kernel as MED, therefore the example in this Figure refers to Mean Multifractal Edge Detector (or shortly Mean-MED) [16]. Figures 3(a-d) show the results obtained from convolving the image with four scales of a Mean kernel: (3×3), (5×5), (7×7), and (9×9) respectively. Figure 3(e) shows the multifractal map that was generated by computing *lfd* from convolved images.

Different Kernels are utilized in the literature [26, 28, 30] for multifractal edge detection, namely Min, Max, OSC, and Edge kernels. Accordingly, using these kernels in local fractal computation generates different edge detectors: Min-MED, Max-MED, Mean-Med, OSC-MED, and Edge-MED respectively. Table 1 summarizes these kernels in a region of size $s \times s$ centered at pixel $I_{x,y}$.

Figure 4 shows how the multifractal edge map is affected by the type of the adopted kernel. It shows the multiscale maps $\{M^1, M^2, M^3, M^4\}$ used to generate the final multifractal edge map using different kernels. As noticed in figures 3 and 4, Mean-MED, Min-MED, and Max-MED provide results that can be easily thresholded to generate a final edge map when compared with OSC-MED and Edge-MED.

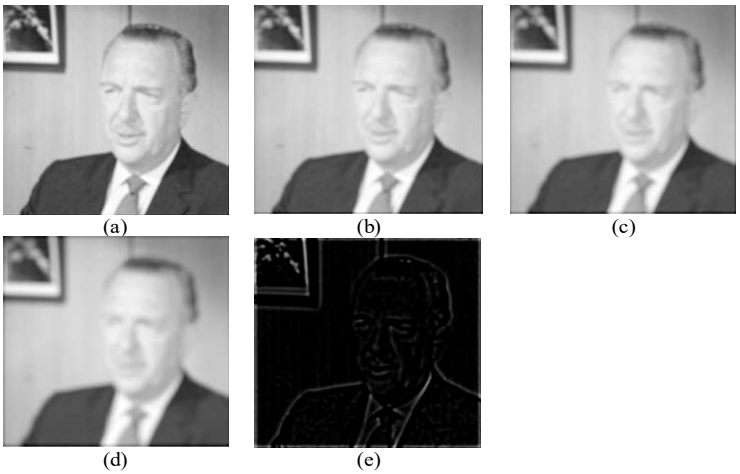

Figure 3: Result of Applying Mean-MED on 'Man' Image in Figure 1(a). a) Multiscale Map M^1 (Kernel Size = 3×3). b) M^2 (Kernel Size = 5×5). c) M^3 (Kernel Size = 7×7). d) M^4 (Kernel Size = 9×9). e) Multifractal Edge Map.

This observation guides our attention to look at the multiscale maps for the Mean, Max, and Min kernels, which can be considered as a kind of regularized or smoothed images. Based on this

ISSN: 1992-8645 www.jatit.org E-ISSN: 1817-3195

observation, we propose the usage of anisotropic diffusion (AD) multiscale filter. It is obviously faster, since it uses gradients in computing the multiscale maps while the specified kernels are nonlinear statistical kernels that run slower in terms of execution time.

Table 1: Well-Known Kernels in Multifractal Analysis.

Kernel Equation	Description
$Min(I_{x,y}) \coloneqq min_{\forall(i,j)\in s}(I_{i,j})$	Min: computes the minimum intensity.
$Max(I_{x,y}) \coloneqq max_{\forall(i,j)\in s}(I_{i,j})$	Max: computes the maximum intensity.
$Mean(I_{x,y}) \coloneqq \sum_{\forall(i,j)\in s}(I_{i,j})/s^2$	Mean: computes the average intensity.
$Edge(I_{x,y}) \coloneqq \sum_{\forall(i,j)\in s}\lvert I_{i,j} - \bar{I}\rvert$, where $\bar{I}$ is the mean for whole image *I*.	Edge: computes the total sum of the absolute differences—resulting from subtracting $\bar{I}$ from each pixel intensity.
$OSC(I_{x,y}) \coloneqq \sum_{\forall(i,j)\in s}\lvert I_{i,j} - \bar{I}_s\rvert$, where $\bar{I}_s$ is the mean of the pixels in an s×s region centered at $I_{x,y}$.	OSC (oscillation): computes the total sum of the absolute differences—resulting from subtracting $\bar{I}_s$ from each pixel intensity.

Figure 4: Results of Applying Min-MED, Max-MED, Edge-MED, and OSC-MED Respectively. a) M^1. b) M^2. c) M^3. d) M^4. e) Multifractal Edge Map.

Journal of Theoretical and Applied Information Technology
15th April 2018. Vol.96. No 7

ISSN: 1992-8645 www.jatit.org E-ISSN: 1817-3195

3. METHODOLOGY

In this paper AD-MED (a multifractal edge detector based on AD filter) is proposed. The main idea is to compute the *lfd* using a set of multiscale regularized maps generated by the AD filter. To this end, the model in figure 5 illustrates the main three stages of the proposed AD-MED, namely: {Applying AD filter, Selecting a set of multiscale maps, Generating the multifractal map}. The last stage generates a local fractal map *E* that is mainly dark with highlighted edges. Details of the model are as follows:

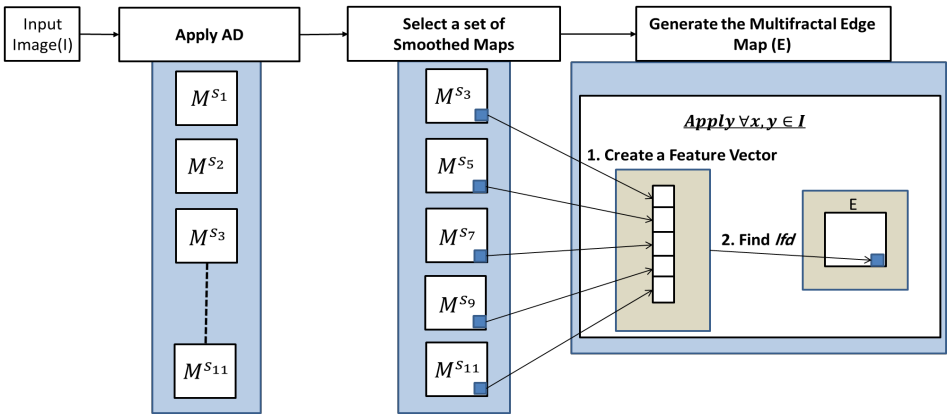

Figure 5: Flow Diagram of the Proposed AD-MED Model.

1. Generate multiscale smoothed versions of the input image using AD filter with *L* iterations, this will generate *L* multiscale images as: $\{M^{s_1}, M^{s_2}, \dots, M^{s_L}\}$, in our experiments we assumed $L = 11$.

2. Select a set of the generated maps: $\{M^{s_3}, M^{s_5}, M^{s_7}, M^{s_9}, M^{s_{11}}\}$.

3. Create a feature vector for each pixel in the image. The feature vector of the pixel $I_{x,y}$ is composed of $\{M^{s_3}_{x,y}, M^{s_5}_{x,y}, M^{s_7}_{x,y}, M^{s_9}_{x,y}, M^{s_{11}}_{x,y}\}$.

4. For each pixel in the position *(x,y)* compute *lfd* as the slope of the most fitted line in a plot of $log(s_i)\ vs\ log(M^{s_i}_{x,y})$, where $s_i \in \{3,5,7,9,11\}$. Repeating this step for all pixels in the image will generate an edge map *E*.

5. Draw the histogram of *E*, and select a threshold α where the histogram converges to zero.

6. The final thresholded (binary) edge map is generated by highlighting edge pixels that are greater than α and suppressing the remaining pixels as defined in eq.7.

$$Binary\ Edge\ Map = \begin{cases} 1, E_{xy} > \alpha \\ 0, E_{xy} \le \alpha \end{cases} \quad (7)$$

The threshold (α) was chosen from the histogram of *E*. Particularly, α is the intensity where the histogram of *E* converges to zero.

4. RESULTS AND ANALYSIS

This section introduces our experimental results and comparisons with other multifractal edge detectors. The comparisons conducted with a set of well-known multifractal edge detectors namely: MIN-MED, MAX-MED, Mean-MED [29], EDGE-MED, and OSC-MED [28]. All experiments are performed using Matlab on a machine with Intel Core i7 CPU running at 2.60GHz and 8GB of RAM.

4.1 Qualitative Evaluation of AD-MED

Qualitative evaluation aims to visually assess the performance of AD-MED when compared to other MEDs. Figure 6 shows that Min-MED, Max-MED, and Mean-MED provide edge maps that can be easily thresholded. However, for Min-MED and Max-MED some undesirable artefacts appear in their results, this is due to the box shape of their structuring element. In addition, Min-MED and Mean-MED tend to produce double edge maps. OSC-MED edge maps are harder to binarize, they mainly depend on manual thresholding as reported in [28]. Edge-MED also has the same problem of binarization and looks

ISSN: 1992-8645 www.jatit.org E-ISSN: 1817-3195

very sensitive to the noise in real images. Results of AD-MED are automatically thresholded as discussed in section 3. AD-MED shows better edge results in terms of edge localization (no double edges in the results). Figure 7 shows more results of AD-MED.

An interesting feature in AD-MED is that it is a multilevel edge detector in a sense that it could be tuned to retrieve edge maps with different levels of details. Figure 8 shows an example where the edge maps are generated by 41 iterations of AD filter. From the 41 multiscale maps $\{M^{s_1}, M^{s_2}, \dots, M^{s_{41}}\}$, AD-MED selected 4 maps to generate the result in figure 8(b); $\{M^{s_{35}}, M^{s_{37}}, M^{s_{39}}, M^{s_{41}}\}$. Figure 8(c) shows an edge map that is generated by selecting the maps $\{M^{s_{15}}, M^{s_{17}}, M^{s_{19}}, M^{s_{21}}\}$, and in figure 8(d) an edge map generated by selecting $\{M^{s_5}, M^{s_7}, M^{s_9}, M^{s_{11}}\}$. As depicted in this figure, the high scale range (Figure 8(b)) means that AD-MED extracted edges from highly regularized images; that's why soft edges are missed in the result. On contrast, the low scale range (Figure 8(d)) means that AD-MED extracted edges from low level regularized images, this insures fine edge preservation.

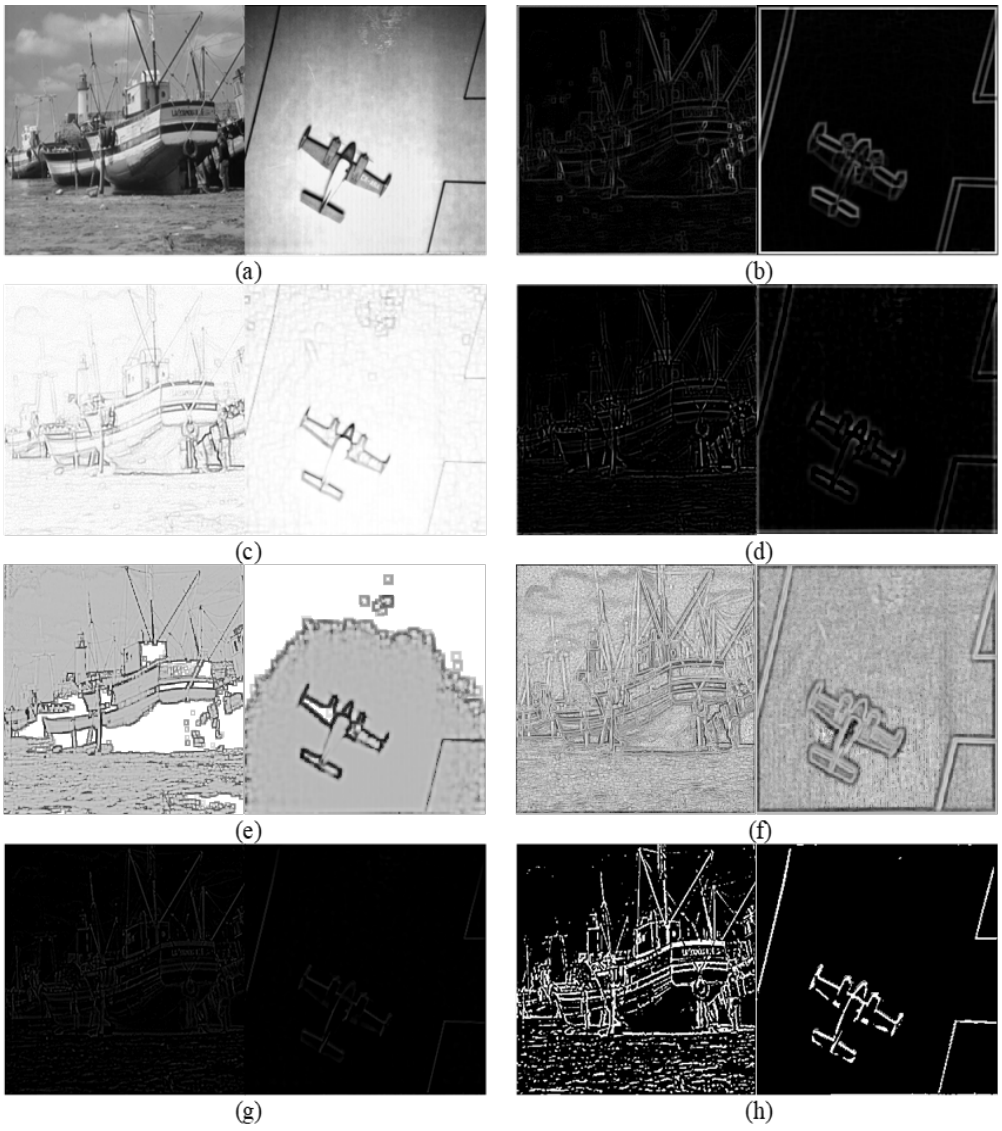

Figure 6: Visual Comparison of Different MEDs. a) Original Images [19]. b) Results of Min-MED. c) Max-MED. d) Mean-MED. e) Edge-MED. f) OSC-MED. g) AD-MED before Thresholding. h) AD-MED after Thresholding.

Journal of Theoretical and Applied Information Technology
15th April 2018. Vol.96. No 7

ISSN: 1992-8645 www.jatit.org E-ISSN: 1817-3195

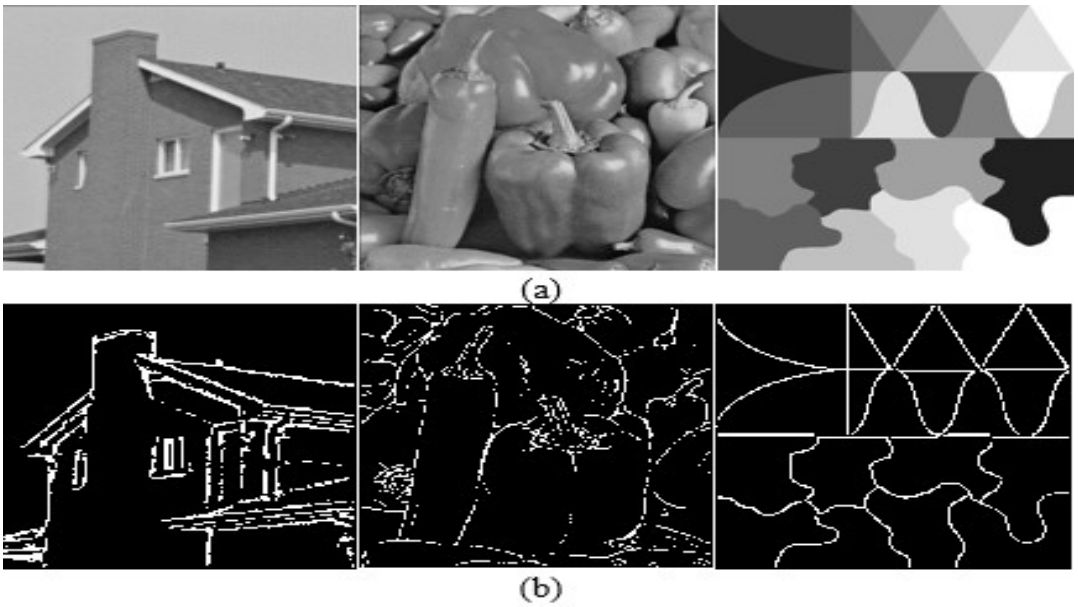

Figure 7: a) Original Images [19]. b) AD-MED Results.

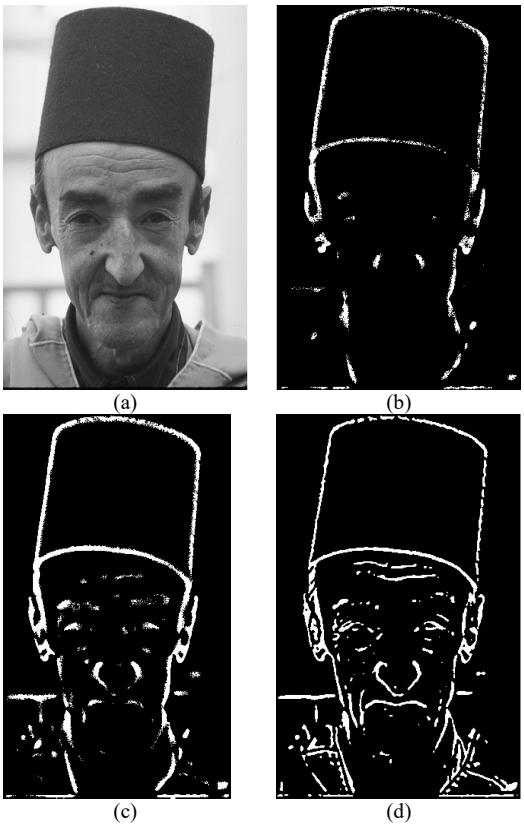

Figure 8: Multilevel Edge Maps Generated Using AD-MED. a) Original Image [31]. b) Edge Map Result Using $\{M^{S_{35}}, M^{S_{37}}, M^{S_{39}}, M^{S_{41}}\}$. *c)* $\{M^{S_{15}}, M^{S_{17}}, M^{S_{19}}, M^{S_{21}}\}$. *d)* $\{M^{S_5}, M^{S_7}, M^{S_9}, M^{S_{11}}\}$.

4.2 Quantitative Evaluation of AD-MED

The quantitative evaluation was conducted to evaluate both the quality and the performance time of the proposed approach.

The first quantitative experiment assesses the quality of our results and compares them with Min-MED, Max-MED, and Mean-MED results. The evaluation metric is the entropy based measure (*Ent*). It is the total sum of the absolute differences—resulting from subtracting the local entropy of a sharpened version of the original image from the local entropy of the original image. The sharpened version of the image is produced using the edge map of a specified edge detector. Herein, a lower value of *Ent* suggests higher information similarity between the original and the sharpened image which means a high quality sharpened image. Accordingly, for the edge detector used in the sharpening procedure, the lower value of this measure insures its better competitive position when compared with other edge detectors. The mathematical notation of this measure is

$$Ent_{(I,Sh)} = \left| \sum_{\forall p \in I} Entropy(I_p) - \sum_{\forall p \in Sh} Entropy(Sh_p) \right| \quad (8)$$

where I is the original image, Sh is the sharpened image of I. I_p is the local patch in I centered at pixel p. Sh_p is the local patch in Sh centered at pixel p. $Entropy(I_p)$ is the entropy of the local patch I_p.

ISSN: 1992-8645 www.jatit.org E-ISSN: 1817-3195

The entropy is defined as [27]

$$Entropy(I_p) = -\sum_{\forall i \in [0,N-1]} P(s_i)\log_2(P(s_i)) \quad (9)$$

where N is the number of gray levels, and $P(s_i)$ is the normalized probability of the gray level s_i. The value of r in this measure was assumed as $r = 11$.

It is worth mentioning that to insure fairness in the comparison, we have compared the results of the edge detectors at fixed number of edges (in our case we have selected the strongest 2000 edge points from each edge map). Then we have applied the sharpening procedure by simply subtracting the edge map from the original image.

Table 2 compares the results of AD-MED with Min-MED, Max-MED, and Mean-MED in terms of *Ent*. The comparison was held on three datasets; UCID dataset (with 1338 images) [32], BSDS500 dataset (with 500 images) [31], and Weizmann dataset (with 100 images) [33]. AD-MED recorded the lowest value and hence it occupies the best ranking position. OSC-MED and Edge-MED are excluded from the comparison because they need manual thresholding. For the Max-MED we inverted its result in order to obtain a dark background and bright edges.

Another experiment was held to compare the execution time for different MEDs. In this experiment AD-MED reported the lowest execution time for different sizes of images. Table 3 shows that on an image of size 100×100, AD-MED is faster than Min-MED, Max-MED, Mean-MED, OSC-MED, and Edge MED by 93.91%, 94.26%, 94.66%, 95.54%, and 91.36% respectively. As well, for an image of size 2000×2000 AD-MED was faster than the specified methods by 91.06%, 91.08%, 95.27%, 96.88%, and 90.49% respectively.

Table 2: Comparison based on Ent Measure.

Dataset	***AD-MED***	***Min-MED***	***Max-MED***	***Mean-MED***
UCID	*1.14E+04*	*1.43E+04*	*1.39E+04*	*1.41E+04*
BSDS500	*7.60E+03*	*1.25E+04*	*1.21E+04*	*1.41E+04*
Weizmann	*2.05E+05*	*2.4E+05*	*2.02E+05*	*2.12E+05*
Overall Datasets	***2.04E+04***	***2.41E+04***	***2.31E+04***	***2.43E+04***

Table 3: Average Execution Time (Seconds) for Different MEDs. For All MEDs, Five Scales are Selected (3,5,7,9,11).

Image Size (pixels)	**Min-MED**	**Max-MED**	**Mean-MED**	**OSC-MED**	**EDGE-MED**	**AD-MED**
100 ×100	1.15	1.22	1.31	1.57	0.81	**0.07**
512×512	11.70	11.57	23.31	25.49	9.57	**0.86**
900×400	13.56	14.34	28.91	34.87	12.53	**1.10**
1500×2000	53.04	55.26	175.81	252.83	91.10	**8.21**
2000×2000	118.63	118.79	224.13	339.82	111.52	**10.60**

5. CONTRIBUTIONS AND SIGNIFICANCE OF WORK

Previous approaches for multifractal edge detection were proposed to build the multifractal edge map by means of statistical kernels which in most cases run slowly and tend to generate some undesirable artefacts in the resulted edge map. In this paper, we showed that the type of the adopted kernel in multifractal approach has a serious impact on the obtained edge map.

Local fractal dimension (*lfd*) is mainly used to analyze the variation in pixel's neighborhood. Despite it is an important issue for pattern recognition applications, the perspective of this study—in relation to multifractal analysis, do not process images based on the exact computation of the local fractal dimension of each pixel, but rather, it advocates a methodology to enforce variations on image edges, while maintaining regularity in their interior regions. This methodology insures clearer multifractal edge maps that can be better thresholded. For this purpose, we proposed anisotropic diffusion filter as a kernel in our model. The obtained edge maps using this model outperform classical MEDs in terms of execution time and quality of results.

Moreover, multifractal binary edge map generation is a difficult task, and (up to our knowledge) there is no research in multifractal edge

ISSN: 1992-8645 www.jatit.org E-ISSN: 1817-3195

detection supports the issue of automatic thresholding of results. Herein, the proposed AD-MED generates an edge map that can be automatically thresholded to discriminate edge from non-edge points.

As a multifractal approach, the incorporation of the scale factor in the computation of *lfd* is an important feature. It is investigated in retrieving different levels of details from the image space, this is achieved by simply tuning the adopted scales in AD-MED.

6. CONCLUSIONS

The new trend of edge detection recommends the incorporation of scale factor in filter design. It is found that multifractal analysis follows this trend through its multiscale analysis that describes the variations in pixel's neighborhood. However, this approach was studied widely for purposes of pattern recognition applications and very few research has been advocated to highlight its abilities in image edge detection.

From the existing work in multifractal edge detection, it was perceived that a set of kernels are used in the literature, most of them are non-linear statistical kernels whose involvement acquires multi-convolution steps that increase the execution time of generating the final edge map. In addition, they tend to produce an edge map that needs manual thresholding to get a final binary result. Besides, some of the kernels tend to produce artefacts according to the shape of the adopted kernel.

Therefore, in this paper, a fast multifractal edge detector AD-MED is proposed. It is a multifractal edge detector that depends on computing the final edge map from a set of smoothed images generated by the anisotropic diffusion (AD) filter. The strength of the proposed AD-MED lies in three points; first, AD is a smoothing filter that preserves edges and does not tend to produce undesirable artefacts in the image. Second, for a small number of iterations, AD-MED is remarkably faster than non-linear statistical kernels, this is because it uses gradients and derivatives while generating smooth images. Third, the resulted edge map can be automatically thresholded.

The evaluation of the proposed edge detector was conducted on three popular datasets: UCID, BSDS500, and Weizmann. Results showed that AD-MED outperforms the existing works, namely: Min-MED, Max-MED, Mean-MED, OSC-MED, and Edge-MED, in terms of quality of the results and execution time. In addition, the incorporation of the scale factor in AD-MED is an important feature that could be investigated in retrieving multilevel edge maps by simply tuning the scales in AD-MED.

As a future work, we plan to extend AD-MED for color images. We also plan to incorporate our edge detector in different image processing applications such as image segmentation, registration and enhancement.

REFERENCES

[1] Ziou D, Tabbone S. "Edge detection techniques-an overview", Pattern Recognition and Image Analysis C/C of Raspoznavaniye Obrazov I Analiz Izobrazhenii, Vol.8, Dec, 1998, pp.537-59.

[2] Panday V, Tiest WM, Kappers AM. "The influence of edges as salient features in haptic shape perception of 3D objects", *World Haptics Conference* (WHC), *2011 IEEE,* 21-24 Jun 2011, Vol.21, pp. 529-532.

[3] Chen Y, Pock T. "Trainable nonlinear reaction diffusion: A flexible framework for fast and effective image restoration", *IEEE transactions on pattern analysis and machine intelligence*, June 2017, Vol.39, No.6, pp.1256-1272.

[4] Chen LC, Barron JT, Papandreou G, Murphy K, Yuille AL. "Semantic image segmentation with task-specific edge detection using cnns and discriminatively trained domain transform", *Proceedings of the IEEE Conference on Computer Vision and Pattern Recognition,* June 2016, pp. 4545-4554.

[5] Liu W, Tian H, Hu J, Cheng S, Yuan H. "Edge Enhanced Traffic Scene Segmentation Algorithm with Deep Neural Network", *SAE Technical Paper*, Sep 23 2017, pp. 1-7.

[6] Haider SA, Khurshid K. "An implementable system for detection and recognition of license plates in Pakistan", *Innovations in Electrical Engineering and Computational Technologies (ICIEECT), International Conference,* 5-7 April 2017, pp. 1-5, Pakistan.

ISSN: 1992-8645 www.jatit.org E-ISSN: 1817-3195

[7] Gonzalez R, Woods R. "Digital Image Processing", 3rd ed. , *Prentice Hall*, 2010.

[8] Oskoei MA, Hu H. "A survey on edge detection methods", *University of Essex*, 2010 29 February, UK.

[9] Schunck BG. "Edge Detection with Gaussian filters at multiple scales", *Proc. IEEE Comp. Soc. Work. Comp. Vis*, 1987, pp.208-210.

[10] Basu M. "Gaussian based edge detection methods -a survey", *IEEE Transactions on Systems, Man, and Cybernetics*, Part C (Applications and Reviews). August 2002, Vol.32, No.3, pp.252-60.

[11] Perona P, Malik J. "Scale-space and edge detection using anisotropic diffusion", *IEEE Transactions on pattern analysis and machine intelligence*. July 1990, Vol.12, No.7, pp.629-639.

[12] Zhang Q, Shen X, Xu L, Jia J. "Rolling guidance filter", *In European Conference on Computer Vision,* September 6 2014, pp. 815-830, Springer, Cham.

[13] Farbman Z, Fattal R, Lischinski D, Szeliski R. "Edge-preserving decompositions for multi-scale tone and detail manipulation", *In ACM Transactions on Graphics* (TOG), August 11 2008, Vol. 27, No. 3, pp. 67. ACM.

[14] Ham B, Cho M, Ponce J. "Robust Guided Image Filtering Using Nonconvex Potentials", *IEEE Transactions on Pattern Analysis and Machine Intelligence*, February 14 2017, Vol.40, No.1, pp.192-207.

[15] Lei T, Fan Y, Wang Y. "Colour edge detection based on the fusion of hue component and principal component analysis", *IET Image Processing*. January 1 2014, Vol.8, No.1, pp.44-55.

[16] Véhel JL. "Introduction to the multifractal analysis of images", *Fisher, Fractal Image Encoding and Analysis,* Springer, 1998, Vol.3, pp. 299–34.

[17] Al-Kadi OS, Watson D. "Texture analysis of aggressive and nonaggressive lung tumor CE CT images". *IEEE transactions on biomedical engineering*. July 2008, Vol.55, No.7, pp.1822-1830.

[18] Tsiotsios C, Petrou M. "On the choice of the parameters for anisotropic diffusion in image processing", *Pattern recognition.* May 31 2013, Vol.46, No.5, pp.1369-1381.

[19] USC Libraries -SIPI Image Database, *http://sipi.usc.edu/database/database.php*, 22/ /December/ 2017.

[20] Falconer K. "Fractal geometry: mathematical foundations and applications", *John Wiley & Sons,* January 9 2004.

[21] Mandelbrot BB. "Fractals: form, chance and dimension", *San Francisco (CA, USA): WH Freeman & Co.,* 1979, Vol.1, No.1, pp. 55-37.

[22] Falconer KJ. "Techniques in fractal geometry", *Chichester (W. Sx.): Wiley*; March 1997.

[23] Creutzburg R, Ivanov E. "Fast algorithm for computing fractal dimensions of image segments", *Recent issues in pattern analysis and recognition*. 1989, Vol.399, pp.42-51.

[24] Lu N. "Fractal imaging", *Morgan Kaufmann Publishers Inc.,* May 1 1997.

[25] Mandelbrot B. "How long is the coast of Britain? Statistical self-similarity and fractional dimension", *Science, May 5* 1967, Vol.156, No.3775, pp.636-8.

[26] Li J, Du Q, Sun C. "An improved box-counting method for image fractal dimension estimation", *Pattern Recognition*, Nov 30 2009, Vol.42, No.11, pp. 2460-2469.

[27] Gray RM. "Entropy and information theory", *Springer Science & Business Media*, January 27 2011.

[28] Paskaš M, Gavrovska A, Jevtić D, Slavković M, Reljin B. "Edge examination using Hölder exponent and image statistics", *Telecommunication in Modern Satellite Cable and Broadcasting Services (TELSIKS), 2011 10th International Conference,* October 5 2011, Vol.1, pp. 329-332.

ISSN: 1992-8645 www.jatit.org E-ISSN: 1817-3195

[29] Paskaš M, Reljin B, Reljin I, Dujković D. "Edge preserved low-pass filtering controlled by local dimension", *Systems, Signals and Image Processing (IWSSIP), 2013 20th International Conference, July 7* 2013, pp. 87-90, IEEE.

[30] Vehel JL, Mignot P. "Multifractal segmentation of images", *Fractals,* September 1994, Vol.2, No.3, pp.371-377.

[31] Martin D, Fowlkes C, Tal D, Malik J. "A database of human segmented natural images and its application to evaluating segmentation algorithms and measuring ecological statistics", *Computer Vision, 2001. ICCV 2001. Proceedings. Eighth IEEE International Conference,* 7-14 July 2001, Vol. 2, pp. 416-423, Canada.

[32] Schaefer G, Stich M. "UCID: An uncompressed color image database". *InStorage and Retrieval Methods and Applications for Multimedia*, December 18 2003, Vol.5307, pp.472-481. International Society for Optics and Photonics.

[33] Alpert S, Galun M, Brandt A, Basri R. "Image segmentation by probabilistic bottom-up aggregation and cue integration", *IEEE transactions on pattern analysis and machine intelligence.* February 2012, Vol.34, No.2, pp.315-327.